



# September 2017 Solar Flare Event: Rapid Heating of the Martian Neutral Upper Atmosphere from the X-class flare as observed by MAVEN

M.K. Elrod<sup>1,2</sup>, S.M. Curry<sup>3</sup>, E.M.B. Thiemann<sup>4</sup>, S. K. Jain<sup>4</sup>

<sup>1</sup>NASA Goddard Spaceflight Center, Greenbelt, MD

<sup>2</sup>CRESSTII, University of Maryland, College Park, MD

<sup>3</sup>Space Science Laboratory, University of California, Berkeley, CA

<sup>4</sup>Laboratory for Atmospheric and Space Physics, University of Colorado, Boulder, CO

Corresponding author: M.K. Elrod, meredith.k.elrod@nasa.gov

## Key points

1. Solar X-class flares rapidly heat the neutral upper atmosphere on timescales similar to the duration of the flare.
2. Scale height enhancements due to the EUV from the flare are higher for O, CO and N<sub>2</sub> than for CO<sub>2</sub> and Ar
3. Responsiveness of the neutral atmosphere to EUV solar flares has implications for atmosphere escape and the early Sun.

## Abstract

On 10 September 2017, the MAVEN mission observed a particularly strong X-class flare. This paper will focus on observations made by NGIMS and the flare response detected by EUVM. We focus the data to the region of the upper atmosphere from 160-300 km and to 10 orbits before and after the flare. The flare peaked near 16:12 UTC with the closest periapsis pass from 17:30 – 17:54 UTC [Lee *et al.*, 2018]. NGIMS measured a significant enhancement in the neutral densities above 195 km for the flare. This enhancement stands out for the major species measured by NGIMS (Ar, CO<sub>2</sub>, CO, O, and N<sub>2</sub>). The correlation of the flare and the enhancement in density and temperature in the upper atmosphere indicates that solar flare heating is most likely the main driver and has important implications for the effects of space weather events on terrestrial atmospheres.

This article has been accepted for publication and undergone full peer review but has not been through the copyediting, typesetting, pagination and proofreading process which may lead to differences between this version and the Version of Record. Please cite this article as doi: 10.1002/2018GL077729

## Introduction

Studies have shown that extreme ultraviolet (EUV, 10-120 nm) irradiance is a critical component to heating of the Martian thermosphere and that events like solar flares, which can quickly deposit significant amounts of energy, can result in rapid heating [Bougher *et al.*, 1999; Liu *et al.*, 2007]. EUV irradiance variability occurs due to the 11-year solar cycle, solar rotation, and solar activity in the form of solar flares. Mars Thermospheric General Circulation Model (MTGCM) indicates that solar EUV/UV heating produces exospheric temperatures of 170 K to 300 K for solar min and solar max respectively [Bougher *et al.*, 2009, 2015]. These modeling studies and the efforts in Fang *et al.*, (2018) suggest that rapid heating is possible during strong solar flare events. The Mars Atmosphere and Volatile Evolution (MAVEN) mission has been collecting data on the Mars upper atmosphere remotely with the Imaging Ultraviolet Spectrograph (IUVS), in combination with solar trends from the Extreme Ultraviolet Monitor (EUVM), and *in-situ* data with the Neutral Gas and Ion Mass Spectrometer (NGIMS) [McClintock *et al.*, 2015; Mahaffy *et al.*, 2014; Jakosky *et al.*, 2015; Eparvier *et al.*, 2015]. Observations thus far include a few extreme class (X-class) flares and dozens of moderate class (M-class) flares since MAVEN arrived [Lee *et al.*, 2017]. Unfortunately for many of the stronger flares at Mars, neutral and EUV observations were not well timed, and for many of these passes the neutral data from the (NGIMS) were not available.

On 10 September, 2017, MAVEN observed the most intense X-class flare to date. Thiemann *et al.*, [2015] reported on the first observations of the heating of the Mars neutral atmosphere due to solar flares. In that study, the 14 largest flares, all magnitude M1 or larger, that had occurred in conjunction with MAVEN *in-situ* observations on the dayside hemisphere were studied. The inferred statistically significant temperature variations from the Ar density scale heights in 3 of the 14 cases with magnitudes of 58K, 64K and 155K focused only on the temperatures derived from the Ar density scale height, which led the authors to conclude that the Mars thermosphere responds and recovers rapidly to heating from solar flares. [Thiemann *et al.*, 2015]. This study found that the 10 September 2017 event produced heating in the upper atmosphere for all major species of ~100K and *in-situ* NGIMS observations were made when the flare was near 25% of its maximum value yet still above the X-class irradiance threshold. With the exception of the smaller flares, and an X-class flare observed during the comet Siding Spring observation campaign, every other flare event had

poor timing with NGIMS observations. Because periapsis observation occurs for 20 minutes every 4.5 hours and typical flares last tens of minutes, obtaining in-situ atmospheric observations during a solar flare can often be missed. The high magnitude (X8.1) of the 10 September 2017 event and the very good timing of the MAVEN periapsis and NGIMS data set up for nearly optimal observations of solar flare heating of the upper atmosphere.

NGIMS is mounted on the Articulated Payload Platform (APP) along with IUVS and Suprathermal and Thermal Ion Composition (STATIC) instrument. During nominal science operations, the APP can be articulated so that the NGIMS 1.5° field of view pointing can be aligned with the ram direction to maximize neutral atmosphere detection. When the APP needs to be re-directed for other operations, NGIMS may still be gathering science; however, if the pointing is off by more than 10° from the ram direction, then incoming signal is too weak for nominal neutral science and the data becomes unreliable. NGIMS can be redirected for a number of reasons: communication passes that require the spacecraft to be pointed towards Earth, IUVS stellar occultations that require special APP pointing during periapsis to focus on specific stars, or NGIMS wind scans that require the instrument to switch to a different science mode. Finally, during solar conjunction due to lack of communication between spacecraft and ground, the APP is fixed for 3 weeks, slowly drifting off ram. During nominal science, NGIMS switches between open source and closed source scanning every orbit. In closed source (CS) mode, NGIMS detects major neutral species (Ar, CO<sub>2</sub>, N<sub>2</sub>, CO, He, O). In open source (OS) mode NGIMS can operate in neutral beaming mode (filament on) to detect atomic neutrals (N, O, C) or ion mode (filament off). NGIMS will alternate between OS ion mode and OS neutral beaming every other orbit. Due to this mode of operations, NGIMS is able to measure neutrals every orbit. The only time NGIMS doesn't have neutral measurements is during non-standard science operations. Communication passes occur twice a week and tend to effect periapsis pointing and NGIMS operations once or twice a week depending on when and where the pass aligns with the orbit. All other special science operations occur approximately once a month for ~10 orbits.

The 10 September 2017 event was unique in that it is the strongest X-class flare, at X8.1, observed since MAVEN arrived at Mars in October 2014 and the second largest in the current 11-year cycle [Thiemann *et al.*, 2018]. Fortunately, neutral NGIMS observations and EUV observations were well timed to coincide with nominal periapsis science.

## Methodology

In order to determine the response of the neutral upper atmosphere due to heating of the neutral upper atmosphere by the X-class solar flare, we extracted NGIMS data for several orbits before and after the flare event. We examined the inbound segment from 350km to 150km and solar zenith angle (sza)  $\sim 67^\circ$  from 2017-09-07 00:49:22 – 2017-09-19 23:22:16 (~55 orbits) around the solar event including the X-class flare around 2017-9-10 16:45 (Figure 1). The Ar data is sorted by density (log scale,  $\text{cm}^{-3}$ ) into bins from 3 to 8 with a step size of 0.2. Displaying the Ar neutral density this way allows us to visualize density changes over time and compare the density topology with the solar transient events in September: the flare, SEPs, and the ICME. For this study we will be focusing on the arrival of the peak of the EUV X-class flare and the correlation of the heating of the atmosphere. Additional features will be studied in later work. Figure 1 illustrates a time series (UTC) of the NGIMS Ar data as a function of altitude (bottom panel) and the EUVM 0-7 nm irradiance (top panel).

Figure 1 has a sharp peak in the Ar neutral densities that corresponds with the arrival of the flare. The gaps in the data are for the communication passes and wind scan. All NGIMS data is from level 2 version 7 revision 3 using both csn and cso neutral abundance files restricted to the inbound only half of the passes. The flare irradiance observations are made using the MAVEN EUVM 0-7 nm band from the level 2 data product version 11 revision 1.

Figure 2 plots the trends for  $\text{CO}_2$ , Ar,  $\text{N}_2$ , CO, O, and the O/ $\text{CO}_2$  ratio vs. altitude for the pre- and post-flare orbits, the average and the flare orbit (5718). The O/ $\text{CO}_2$  ratio is lower at a given altitude for the flare orbit due to the higher  $\text{CO}_2$  densities produced. However, the steeper O scale height than  $\text{CO}_2$  is indicative of higher production of O due to photochemistry and cooling of  $\text{CO}_2$  by radiative transfer. The ratio is lower because the heating is deposited lower in the atmosphere and dispersed higher in the atmosphere and causes the O/ $\text{CO}_2$  crossover point to raise, where O is more abundant in the atmosphere than  $\text{CO}_2$ , to be higher in altitude [Fang *et al.*, 2018, Bougher *et al.*, 1999]. The solar flare peak occurred at 2017-09-10 16:12 UTC, which preceded the MAVEN periapsis 5718 at 17:38 UTC by ~70 minutes. To focus on neutral data trends near the flare, we examined data from 2017-09-08 16:44:08 orbit 5714 to 2017-09-12 13:50:54 orbit 5724. The average orbit-to-orbit variations in density in the Martian atmosphere can vary by factors of  $\sim 1.35 - 2.75$  on the dayside within

the same solar conditions due to nominal structure and variations in the atmosphere (e.g. waves and tides). In order to compare the heating from the solar event versus the average orbit to orbit variations we compared the flare orbit 5718 with several orbits before and after (Figure 2). The densities for orbit 5718 (green line) are greater than the pre-flare (solid black line) and post-flare (dashed black line) at 225 km on average by a factor of 4.95 for CO<sub>2</sub>, 3.72 for Ar, 2.62 for N<sub>2</sub>, 2.7 for O, and 2.9 for CO. This is significantly higher than the orbit to orbit variations. This temperature change of ~102 K (see table 1) as measured with Ar is greater than the average for at this altitude for day/night difference seen at Mars which is closer to ~3.2.

From Figure 2 it is clear that the density increases significantly at the higher altitudes due to warming and changing scale height. We computed the changes in temperature by fitting scale height to the log(density) vs. altitude. Because the density changes so significantly over altitude it was clear that we could not make an isothermal assumption for large altitude ranges. Instead we performed piece-wise linear fits to the neutral density scale heights (see Table 1), over smaller altitude ranges that conformed to the isothermal assumption more accurately. Figure 3 shows the scale height fits for each of these segments and each of the major species (Ar, CO<sub>2</sub>, and N<sub>2</sub>) in the left panel. The right panel plots the pre-flare, flare and post-flare N<sub>2</sub>, Ar and CO<sub>2</sub> computed temperatures based on these scale heights. N<sub>2</sub> and Ar have the highest increase in temperature at the highest altitude, while CO<sub>2</sub> is shallowest. Ar being the least reactive species is the best indicator of the atmospheric temperature. Scale height and temperature are computed using the density definition for scale height (1) and (2). Getting a linear fit of log(density) vs altitude will produce a slope equal to the scale height that can be turned into a temperature.

$$H = \frac{kT}{m_s g} \quad (1)$$

$$\rho = \rho_0 e^{-\int_0^z dz/H} \quad (2)$$

Where z is altitude, T is temperature H is scale height,  $\rho$  is density, and  $\rho_0$  is the density at a reference altitude,  $m_s$  is mass of the individual species, and k is the Boltzmann constant. Combining equations (1) and (2) leads to using  $H = -\Delta z / \ln(\rho/\rho_0)$  for linear fit over isothermal altitude ranges.

The temperatures not only increased more at higher altitudes for N<sub>2</sub>, and Ar, but also when compared with the pre- and post-flare average temperatures. We also computed the low, middle, upper, and top scale heights and temperatures for the pre- and post-flare average flare composition for comparison. The greatest heating occurred from pre-flare to flare of approximately 100K for Ar and 120K for N<sub>2</sub> in the upper and top ranges in the exobase range (185-215km and 215-260km respectively). O and CO densities saw a significant increase in both associated temperature and scale height (see table 1) and larger than those of Ar. This is likely due to photochemical changes [Thiemann *et al*, 2018], making it difficult to compute a temperature for O and CO at these altitudes. In these ranges the following heating and cooling for each species occurred: above ~180km, collisions become increasingly rare, and the various species are not in thermal equilibrium. CO<sub>2</sub> likely did not heat as much as the Ar and N<sub>2</sub> because there is the possibility that it can cool quicker due to vibrational modes. These temperature changes are similar to rapid heating and cooling by solar flares as previously observed [Thiemann *et al.*, 2015]. These numbers likely could have been higher had the periapsis pass started sooner.

Table 1 gives the pre-flare, flare, and post-flare densities, scale heights and derived temperatures for Ar, CO<sub>2</sub>, N<sub>2</sub>, O and CO. The key to note on CO and O temperatures is that these are derived from the scale heights and are not actual atmospheric temperatures. Because O and CO density changes are more strongly influenced by photochemical processes in the atmosphere O and CO are not good indicators for atmospheric temperature. Ar and N<sub>2</sub> as non-reactive species are the best indicators for actual atmospheric temperature. While CO<sub>2</sub> temperature was in good agreement with Ar and N<sub>2</sub> before and after the flare, as is typical, it was only during the intense heating of the flare that we saw lower temperature for CO<sub>2</sub> while the rest of the atmosphere heated much more rapidly. This difference likely could be due to the capacity of CO<sub>2</sub> to radiatively cool [Bougher and Roble, 1991]. Additional modeling efforts will be needed to explore these concepts. Using the Ar and N<sub>2</sub> temperatures as a measure of how much the exosphere heated from the solar flare, Ar saw heating of ~100K and N<sub>2</sub> saw heating of ~120K.

## Discussion

Previous studies of the effects of intense X-class EUV solar flares on the terrestrial upper atmosphere found that the neutral atmosphere experiences rapid heating and cooling

coupled with the plasma heating and cooling on a faster timescale [Liu *et al.*, 2007]. Timescale predictions from these previous observations indicate that the neutral atmosphere should experience a rapid heating correlated with the arrival of the peak of the flare and this heating will dissipate within an hour of the flare passing. The peak of the flare on 10 September 2017 arrived at 16:12UTC and the flare emission at the high intensity level lasted for ~45 min. The MAVEN periapsis pass began at 17:30UTC. Had the periapsis pass been as much as an hour later, starting after the end of the duration of the flare, it is likely NGIMS would not have been able to observe the neutral atmosphere heating due to the flare arrival because the atmosphere cools rapidly.

MAVEN IUVS made scans lower in the atmosphere at slightly higher  $sza \sim 85^\circ$  than NGIMS measurements [Jain *et al.*, 2018]. IUVS found substantive heating in the atmosphere below the exobase at ~170km. As this is the lower limit for the observations for NGIMS it becomes complimentary to track the heating in the upper atmosphere. IUVS and NGIMS have pointing offset by about  $90^\circ$  due to mounting on the APP. Due to instrumentation limitations the NGIMS data is less reliable on outbound portion of the passes [Benna and Elrod, 2016]. IUVS observed temperatures that show a strong latitudinal gradient with flare temperature. Perturbations are limited from low to mid-latitudes (up to  $30^\circ$ ) in the inbound leg of the MAVEN orbit [Jain *et al.*, 2018]. NGIMS observations ran from 300km to 150km from  $20^\circ - 40^\circ$  latitude during the inbound portion of the periapsis pass and only crossing  $30^\circ$  after getting below 200km. During periapsis because of mounting and science constraints (IUVS and NGIMS are pointed  $90^\circ$  offset) they observe different portions of the atmosphere and provide complimentary information of the neutral response of the Martian neutral upper atmosphere.

Solar events including flares can have significant impacts on the Martian thermosphere; this has significant implications for understanding how space weather events drive atmospheric escape [Brain *et al.*, 2015; Curry *et al.*, 2015; Jakosky *et al.*, 2015; Thiemann *et al.*, 2015; 2018; Jain *et al.*, 2018]. These planetary ions can also precipitate back into the upper atmosphere and collide with neutrals, giving them enough energy to escape Mars' gravitational well- a process called sputtering [Johnson *et al.*, 1998; Leblanc *et al.*, 2002]. Sputtering is believed to have been the main driver of atmospheric loss early in Mars' history [Luhmann *et al.*, 1992] yet is a much less significant process today (in comparison to photochemical escape of O). NGIMS observed a strong response in the neutral atmosphere

due to the flare, the effects of other solar effects on the neutral atmosphere appear to be less significant but more data is still needed. Because solar cycle 24 has been extremely quiet with respect to space weather [Curry *et al.*, 2018], the question of how solar transients may have affected the Martian atmosphere with respect to flares and other solar events during earlier epochs of the Sun, when it was significantly more active, is a subject to be explored further.

### **Summary & Conclusion**

Heating in the upper atmosphere of Mars is dominated by solar EUV energy deposition. NGIMS scale height analysis reveals that, after the peak of an X-Class solar flare, both  $N_2$  and Ar appear to heat more readily than  $CO_2$  in response to this flare event and because Ar is inert, it is the best indicator of the temperature of the atmosphere. The significant increase of the Ar temperature in the upper atmosphere is a good indicator that the whole atmosphere was heated due to solar EUV. Figure 2 and 3 both show that the temperature changes for  $CO_2$ , while significantly increasing above 180km, was significantly less than the temperature changes for O. Since O production is a by-product of ionization its scale height steepens with the addition of more O atoms. See Thiemann *et al.*, [2018] for the implications of increased O production has on the ionosphere. IUVS data indicated that the atmospheric heating began to drop off by the outbound pass [Jain *et al.*, 2018]. Additionally, NGIMS only observed the response of the upper neutral atmosphere to the flare. The response of the neutral upper atmosphere to the September 2017 flare suggests that the more intense and frequent x-class flares during earlier epochs of the sun may have been a powerful driver of neutral heating and atmospheric escape, and furthermore may have implications for exoplanetary atmospheres with more active stellar hosts.

### **Acknowledgment**

All data used in this work is published in the Planetary Data System (<https://pds.jpl.nasa.gov>). We used NGIMS level 2 v07 r03 neutral data (csn and cso files), and EUVM level 2 version 11 revision 2 all available on the PDS. The NGIMS data is available on the PDS atmospheres node and the EUVM is available on the PPI node. Significant events like flares are listed on the MAVEN Science Data Center public site under mission events (<https://lasp.colorado.edu/maven/sdc/public>). This work is supported by the MAVEN mission, NASA GSFC, LASP, and SSL Berkeley. Primary funding through CRESST II cooperative agreement CA 80GSFC17M0002.

## References

- Benna, M., M.K.Elrod, NGIMS PDS Software Interface Specification, [https://pds-atmospheres.nmsu.edu/data\\_and\\_services/atmospheres\\_data/MAVEN/ngims.html](https://pds-atmospheres.nmsu.edu/data_and_services/atmospheres_data/MAVEN/ngims.html)
- Bougher, S. W., S. Engel, R.G.Roble, B. Foster, Comparative terrestrial planet thermospheres 2. Solar cycle variation of global structure and winds at equinox, *JGR Vol 104*, no. E7, pp 16591 – 16611, Jul 1999.doi:[10.1029/1998JE001019](https://doi.org/10.1029/1998JE001019)
- Bougher, S.W, R.G. Roble, Comparative terrestrial planet thermospheres. I - Solar cycle variation of global mean temperatures (1991), *J.Geophys. Res. Planets*, (ISSN 0148-0227), vol. 96, July 1, 1991, p. 11,045-11,055.[10.1029/91JA01162](https://doi.org/10.1029/91JA01162)
- Bougher, S. W., T. M. McDunn, K. A. Zoldak, and J. M. Forbes (2009), Solar cycle variability of Mars dayside exospheric temperatures: Model evaluation of underlying thermal balances, *Geophys. Res. Lett.*, **36**, L05201, doi:[10.1029/2008GL036376](https://doi.org/10.1029/2008GL036376).
- Bougher, S. W., D. Pawlowski, J. M. Bell, S. Nelli, T. McDunn, J. R. Murphy, M. Chizek, and A. Ridley (2015), Mars global ionosphere-thermosphere model: Solar cycle, seasonal, and diurnal variations of the Mars upper atmosphere, *J. Geophys. Res. Planets*, **120**, 311–342, doi:[10.1002/2014JE004715](https://doi.org/10.1002/2014JE004715).
- Brain, D. A., et al. (2015), The spatial distribution of planetary ion fluxes near Mars observed by MAVEN, *Geophysical Research Letters*, n/a-n/a, doi:[10.1002/2015gl065293](https://doi.org/10.1002/2015gl065293).
- Eparvier, F. G., P. C. Chamberlin, T. N. Woods, and E. M. B. Thiemann (2015), The solar extreme ultraviolet monitor for MAVEN, *Space Science Reviews*, **1-9**, doi:[10.1007/s11214-015-0195-2](https://doi.org/10.1007/s11214-015-0195-2).
- Fang, Xiaohua, D. Pawlowski, Y.J. Ma, E. M. B Thiemann, C. Dong, S. Bougher, F. Eparvier, D. Brain, C.O. Lee, Y.X., Dong, P. Chamberlin, M. Benna, M.K. Elrod, W.B. Wang, P. Mahaffy, B. Jakosky, (2018) Global Simulations of Mars upper atmospheric effects of the 10 September 2017 solar flare, *GRL*, submitted #2018GL077829
- Jakosky, B. M., R. P. Lin, J. M. Grebowsky, J. G. Luhmann, D. F. Mitchell, G. Beutelschies, and F. Lefèvre (2015), The Mars Atmosphere and Volatile Evolution (MAVEN) mission, *Space Science Reviews*, **1-46**, doi:[10.1007/s11214-015-0139-x](https://doi.org/10.1007/s11214-015-0139-x).

Jain, S. K., J. Deighan, N.M. Schneider, A.I. Stewart, J.S. Evans, E.M.B. Thiemann, M.S. Chaffin, M.Crismani, M.H.Stevens. M.K.Elrod, A.Stiepen, W.E. McClintock, D.Y. Lo, G.M. Holsclaw, J.T. Clarke, F.G., Eparvier, P.C. Chamberlin, F. Lefevre, F. Montemessin, B.M. Jakosky, "Response of Martian thermosphere to the X8.2 solar flare of 10 September 2017 as seen by MAVEN/IUVS" *GRL*, submitted #2018GL077731

Johnson, R. E., D. Schnellenberger, and M. C. Wong (2000), The sputtering of an oxygen thermosphere by energetic O<sup>+</sup>, *Journal of Geophysical Research: Planets*, 105(E1), 1659-1670, doi:10.1029/1999JE001058.

Lee, C. O., Hara, T., Halekas, J. S., Thiemann, E., Chamberlin, P., Eparvier, F., ... & Gruesbeck, J. (2017). MAVEN observations of the solar cycle 24 space weather conditions at Mars. *Journal of Geophysical Research: Space Physics*, 122(3), 2768-2794.

Lee, C. et al., "Observation and Impacts of the 10 September 2017 Solar Events at Mars: An Overview", submitted

Leblanc, F., and R. E. Johnson (2002), Role of molecular species in pickup ion sputtering of the Martian atmosphere, *Journal of Geophysical Research*, 107(E2), doi:10.1029/2000je001473.

Liu, Huixin, Hermann Lühr, Shigeto Watanabe, Wolfgang Köhler, and C. Manoj, Contrasting behavior of the thermosphere and ionosphere in response to the 28 October 2003 solar flare, *JGR*, vol. 112, a07305, 2007, doi:10.1029/2007JA012313,

Lollo, A., P. Withers, K.Fallows, Z. Girazian, M. Matta, and P.C. Chamberlain (2012), "Numerical simulations of the ionosphere of Mars during a solar flare", *J Geophys. Res.*, 117(A5), 2156-2202, doi:10.1029/2011JA017399,a05314.

Luhmann, J. G., R. E. Johnson, and M. H. G. Zhang (1992), Evolutionary impact of sputtering of the Martian atmosphere by O<sup>(+)</sup> pickup ions, *Geophysical Research Letters* 19(21), 2151-2154, doi:10.1029/92gl02485.

Mahaffy, P. R., et al. (2014), The neutral gas and ion mass spectrometer on the mars atmosphere and volatile evolution mission, *Space Science Reviews*, **1-25**, doi:[10.1007/s11214-014-0091-1](https://doi.org/10.1007/s11214-014-0091-1).

McClintock, W.E., N.M. Schneider, G.M.Holsclaw, J.T. Clarke, A.C. Hoskins, I.Stewart, F. Montmessin, R.V. Yelle, and J.Deighan (2015), The Imaging Ultraviolet Spectrograph (IUVS) for the MAVEN Mission, *Space Sci. Rev.*, 195, 75- 124, doi:[10.1007/s11214-014-0098-7](https://doi.org/10.1007/s11214-014-0098-7)

Mendillo, M., P. withers, D. Hinson, H Rishbeth, and B. Reinisch (2006), “Effects of Solar Flares on the Ionosphere of Mars”, *Science*, 311, 1135-1138, doi:[10.1126/science.1122099](https://doi.org/10.1126/science.1122099).

Qian, L., A.G. Burn, P.C. Chamberlain, and S.C. Solomon, (2011), “Variability of thermosphere and ionosphere responses to solar flares”, *J. Geophys. Res.* 116(A10), 2156-2202, doi: [10.1029/2011JA016777](https://doi.org/10.1029/2011JA016777),a10309.

Thiemann, E.M.B, F. G. Eparvier, L. A. Andersson, C. M. Fowler, W. K. Peterson, P. R. Mahaffy, S. L. England, D. E. Larson, D. Y. Lo, N. M. Schneider, J. I. Deighan, W. E. McClintock, and B. M. Jakosky, Neutral density response to solar flares at Mars, *GRL*, 42, 8986–8992, 2015 doi:[10.1002/2015GL066334](https://doi.org/10.1002/2015GL066334).

Thiemann, E.M.B, L.A. Andersson, R. Lillis, P. Withers, S. Xu, M. Elrod, S. Jain, D. Pawlowski, P.C. Chamberlin, F.G. Eparvier, M. Benna, C. Fowler, M.D. Pilinksi, S. Curry: The Mars Upper Ionosphere Response to the X8.2 Solar Flare of 10 September 2017, *GRL*, submitted.#2018GL07730

Table 1: Changes in scale heights and temperatures of key species for the pre-flare, flare and post-flare data.

Species	Altitude range (km)	Density at 180 km (cm <sup>-3</sup> )	Density at 225 km (cm <sup>-3</sup> )	Scale Height (lower, upper) km	Temperature (lower, upper) K
CO <sub>2</sub>	156 – 240	1.013e8	1.005e6	10.1968	179.34
	155 – 170	1.570e8	4.465e6	Lower: 10.4984	Lower: 184.65
	170 – 182			Middle: 10.5796	Middle: 186.07
	182 – 198			Upper: 12.2129	Upper: 214.80
	198 – 253			Top: 12.6252	Top: 222.05
155 – 246	1.065e8	1.234e6	10.2678	180.60	
Ar	155 – 231	3.74e6	1.023e5	11.9841	191.62
	154 – 171	5.143e6	3.558e5	Lower: 11.4820	Lower: 183.59
	171 – 183			Middle: 11.6313	Middle: 185.97
	183 – 196			Upper: 13.8056	Upper: 220.74
	196 – 259			Top: 18.3535	Top: 293.46
155 – 236	3.759e6	1.254e5	12.5323	200.38	
N <sub>2</sub>	155 – 249	2.955e7	2.421e6	17.0880	191.26
	155 – 175	3.375e7	5.823e6	Lower: 17.3343	Lower: 194.01
	175 – 192			Middle: 19.7742	Middle: 221.32
	193 – 211			Upper: 26.5137	Upper: 296.75
	211 – 256			Top: 28.5043	Top: 319.03
154 – 257	3.077e7	2.739e6	17.8332	199.60	
CO	155 – 252	1.001e7	6.37e5	15.6125	N/A
	155 – 179	1.222e7	1.666e6	Lower: 14.7902	N/A
	179 – 196			Middle: 18.0427	
	197 – 214			Upper: 23.0809	
	214 – 257			Top: 26.6994	
154 – 257	1.082e7	7.498e5	16.2752	N/A	
O	154 – 253	4.177e7	5.465e6	21.3235	N/A
	153 – 170	4.614e7	1.299e7	Lower: 20.6190	N/A
	170 – 181			Middle: 21.0454	
	182 – 194			Upper: 28.6492	
	192 – 259			Top: 36.7744	
154 – 266	4.945e7	6.766e6	22.1749	N/A	

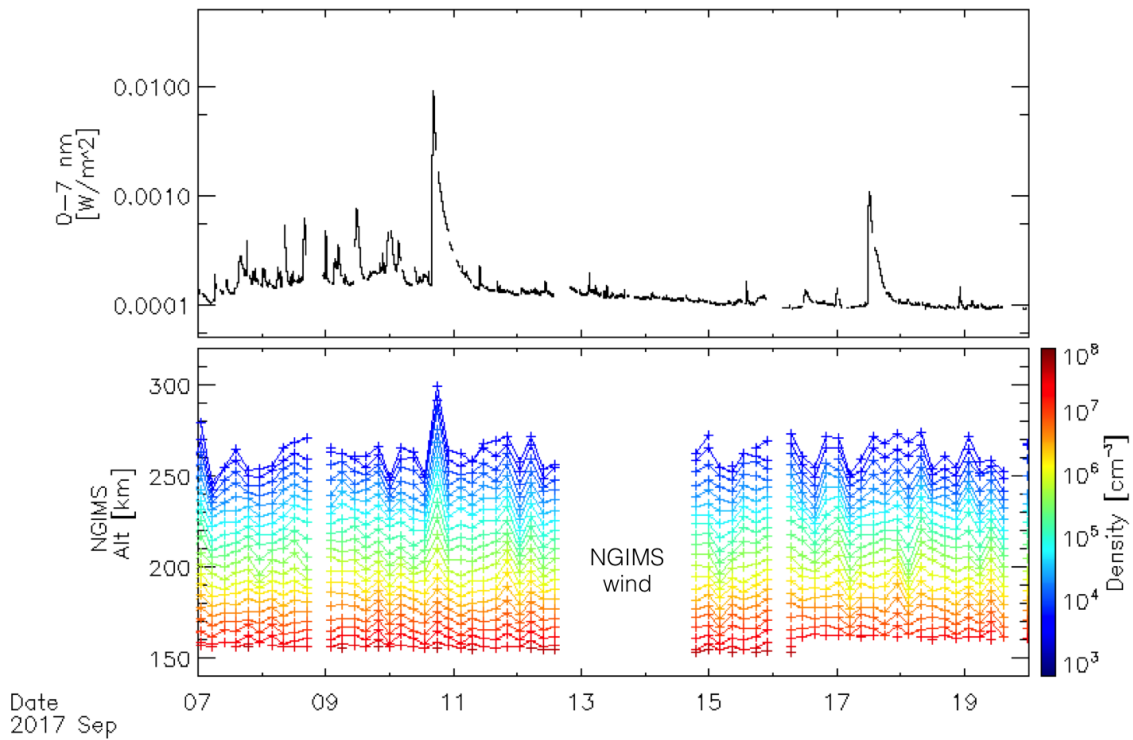


**Figure 1**

Comparison of EUVM measurements showing the approach of the flare (top panel) for the 0-7 nm range along with the NGIMS Ar density (bottom panel) for the time frame of the flare. NGIMS density is binned by density ( $\log, \text{cm}^{-3}$ ) and plotted as altitude vs time. Each line represents a density contour.

Accepted

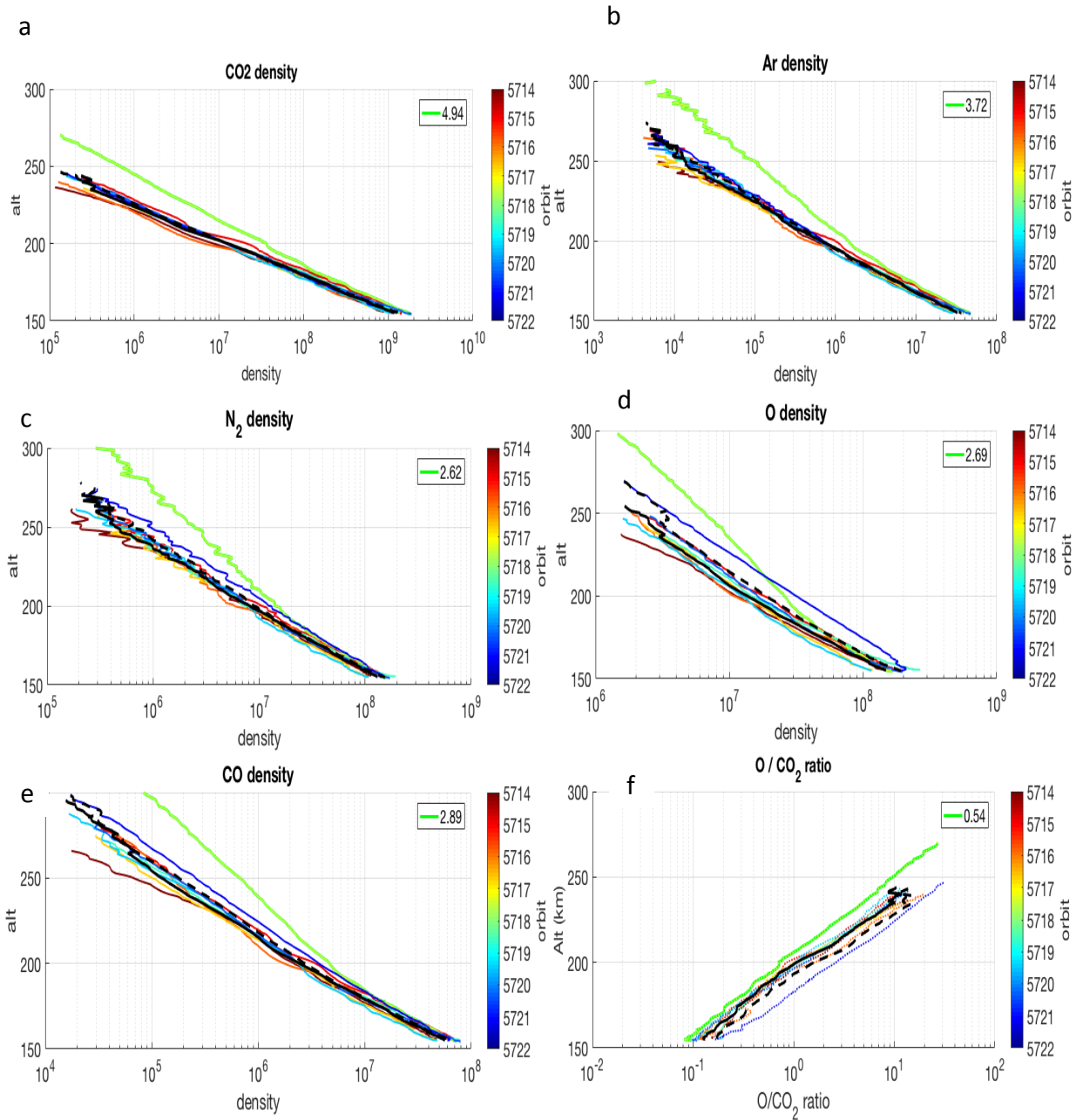


**Figure 2**

Altitude and Density profiles from pre-flare (red-yellow) and post-flare (teal-blue) orbits. The flare orbit (5718) is in green and the enhancement factor over the orbit to orbit variability has been computed for each species at 225km. (a) CO<sub>2</sub> densities orbit 5718 (green) is enhanced by a factor of ~5, (b) Ar densities orbit 5718 (green) is enhanced by a factor of ~4, (c) N<sub>2</sub> densities orbit 5718 (green) is enhanced by a factor of ~2.7, (d) O densities orbit 5718 (green) is enhanced by a factor of ~2.7, (e) CO densities orbit 5718 is enhanced by a factor of ~3 and (f) while O has a steeper scale height due to photochemistry, more CO<sub>2</sub> is produced vs altitude causing the O/CO<sub>2</sub> ratio to be lower by a factor of 0.54 at 225km.

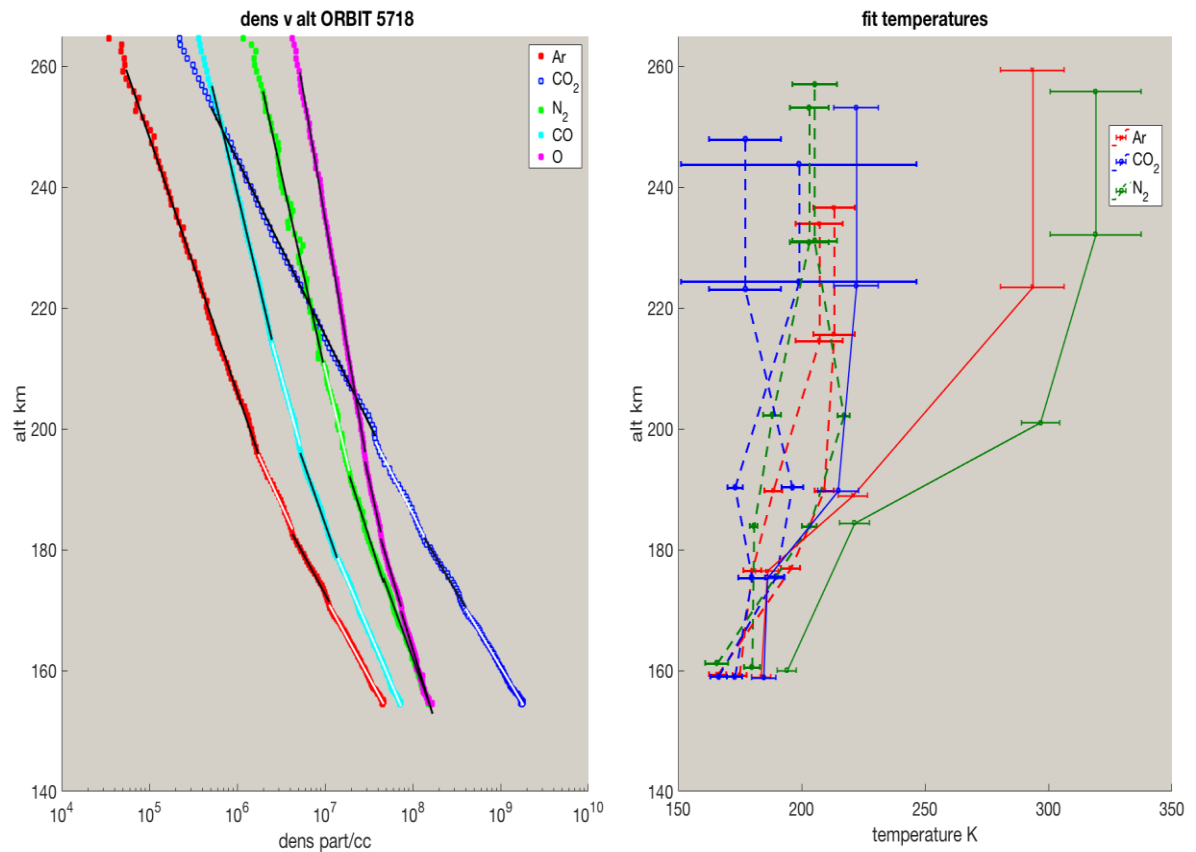


**Figure 3**

Left: Ar (red), CO<sub>2</sub> (blue), N<sub>2</sub> (green), CO (cyan) and O (magenta) density vs altitude scale height fits (left panel) and derived temperatures. Right: The temperature computed from the scale height fits for CO<sub>2</sub> (blue) Ar (red), and N<sub>2</sub> (green) for the pre- and post-flare (dashed) and flare (solid) orbits. The changes in the temperature are higher at the higher altitudes, particularly over 185 km for N<sub>2</sub> and Ar.

Accep